

**OPTICAL MULTIPLEXING FOR HIGH-THROUGHPUT  
SPECTROSCOPIC ANALYSIS**

A Senior Scholars Thesis

by

SAADIAH GUL AHMED

Submitted to Honors and Undergraduate Research  
Texas A&M University  
in partial fulfillment of the requirements for the designation as

UNDERGRADUATE RESEARCH SCHOLAR

May 2012

Major: Electrical Engineering

**OPTICAL MULTIPLEXING FOR HIGH-THROUGHPUT  
SPECTROSCOPIC ANALYSIS**

A Senior Scholars Thesis

by

SAADIAH GUL AHMED

Submitted to Honors and Undergraduate Research  
Texas A&M University  
in partial fulfillment of the requirements for the designation as

UNDERGRADUATE RESEARCH SCHOLAR

Approved by:

Research Advisor:  
Associate Director, Honors and Undergraduate Research:

Michael J. McShane  
Duncon MacKenzie

May 2012

Major: Electrical Engineering

## **ABSTRACT**

Optical Multiplexing For High Throughput Spectroscopic Analysis. (May 2012)

Saadiah Gul Ahmed  
Department of Electrical Engineering  
Texas A&M University

Research Advisor: Dr. Michael J. McShane  
Department of Biomedical Engineering

Implantable optical biosensors are being developed as aids for medical monitoring. Such optical biosensors are analyzed for performance in dynamic sensor testing environment. Multi-Frequency Phase Fluorometer (MFPF) is a key measuring device of dynamic sensor testing. In current laboratory setup, this device can accommodate single sensor testing at a time. In this research work, an optical multiplexer (MUX) was designed and built to enable simultaneous testing of multiple optical biosensors using a single MFPF. Several MUX designs were objectively evaluated and the most effective design in terms of cost, efficiency, optical attenuation losses and scalability was selected for development. The MUX prototype enabled concurrent testing of three biosensor samples, however, the number of samples can be further scaled up. It was found that the MUX can provide adjustable temporal resolution and precise alignment repeatability with minimal data loss during an experiment. The MUX expanded the capabilities of the existing setup by allowing testing of multiple sensors with a single MFPF resulting in significant cost reduction. The cost analysis showed that this solution can reduce equipment cost by twelve times for the same throughput. In addition, the MUX allowed direct comparison of sensors without the need of correcting for variations in testing with

multiple MFPPs. The proposed design approach is a significant contribution in optical biosensor testing as it provides greater throughput and scalability while being an economical and compact solution.

## **NOMENCLATURE**

MFPF	Multi Frequency Phase Fluorometer
MUX	Multiplexer
LED	Light Emitting Diode
DIO	Digital Input/Output
DAQ	Data Acquisition

## TABLE OF CONTENTS

	Page
ABSTRACT .....	iii
NOMENCLATURE .....	v
TABLE OF CONTENTS .....	vi
LIST OF FIGURES .....	viii
LIST OF TABLES .....	x
 CHAPTER	
I INTRODUCTION .....	1
Background .....	1
Sensor testing apparatus .....	3
Research motivation .....	5
Options for multiple sensor testing .....	7
Project objective .....	8
II MATERIALS AND METHODS .....	9
Multiplexing and demultiplexing .....	9
Functionality of optical MUX .....	10
Selection of the two MUX parts .....	13
Final configuration of optical MUX .....	24
Methods for testing the MUX performance .....	26
III RESULTS .....	31
Efficiency test .....	31
Distance test .....	33
Motion control test .....	35
IV DISCUSSION AND CONCLUSION .....	37
Benefits of MUX over MFPP .....	37
Conclusion .....	38

REFERENCES.....	39
CONTACT INFORMATION.....	40

## LIST OF FIGURES

FIGURE	Page
1 Schematic of enzymatic microparticle sensor and accompanying confocal micrograph depicting indicator (PtOEP, blue) and reference (RITC, pink) dye location .....	2
2 Schematic of dynamic testing apparatus used to quantify sensor response properties .....	3
3 A single channel MFPP manufactured by Tau Theta with Ocean Optics bifurcated optical fiber .....	4
4 A portion of dynamic sensor testing apparatus containing the MFPP, optical fiber and the reaction chamber. ....	5
5 Comparison of the actual glucose concentrations exposed to the sensors and the predicted glucose level based on the sensor response .....	6
6 Multiplexing and demultiplexing by the optical MUX .....	10
7 Divergence of light as it leaves the input optical fiber .....	12
8 Efficient transfer of light by plano-convex lenses from input to output fiber.....	14
9 Efficient transfer of light by a lens between input and output fiber .....	15
10 All optical elements integrated together to form one channel of the Optics Section .....	16
11 Linear actuator built from a lead screw attached to a motor .....	19
12 Concept of a rotational device based on reduction gear method.....	21
13 Transfer of light between the fibers through reflection of a mirror .....	22
14 The final configuration of Motor Control Unit .....	24
15 Schematic of Optical Section and Motion Control Unit integrated together to make up an optical MUX .....	25
16 Setup for measuring reference value .....	27



FIGURE	Page
17 Experimental setup for measuring light through one of the MUX channels. ....	29
18 Experimental setup for the Motion Control test .....	30
19 Graph of intensity (number of counts) and efficiency (%) at five data points.....	32
20 Divergence of light with increasing distance .....	33
21 Bar chart of average efficiency at three distances between channels.....	34
22 Graph of intensity versus time for the Motion Control test .....	36

## LIST OF TABLES

TABLE	Page
1 Optical elements for the Optics Section .....	17
2 Sampling variables for the Efficiency test .....	33
3 Average efficiency at three distances .....	35

# CHAPTER I

## INTRODUCTION

### Background

Biosensors are detection devices that can monitor changes in biological analytes found in interstitial fluid. In medical research, dermally implantable optical biosensors are being developed as minimally invasive approach for biochemical monitoring in patients. These optical biosensors act as “smart tattoos” that contain different types of micro-scaled luminescent particles [1]. Based on competitive ligand-analyte binding or substrate-specific enzymatic reactions, the luminescence response of these sensors, once implanted, can be monitored noninvasively using excitation light [1].

In the BioSyM Laboratory at Texas A&M University, sensor prototypes intended for implantation and based on enzymatic reactions are being pursued for diabetic glucose sensing. One such example is of an enzyme called glucose oxidase (GOx) that converts glucose in presence of molecular oxygen and water into gluconic acid and hydrogen peroxide [1]. Oxygen concentration levels that are proportional to glucose can be then optically monitored by a phosphorescent dye, such as Pt(II) octaethylporphine (PtOEP), enabling an indirect measurement for glucose [1]. In this example, the enzymatic sensor

---

This thesis follows the style of *Journal of Biomedical Optics*.

is prepared by immobilizing the dye (which is quenched by oxygen) and glucose oxidase in hybrid silicate microsphere that is coated with nanofilm and reference dye (RITC) (Fig. 1) [2]. The phosphorescent dye is excited by a green light from a LED (light emitting diode) to emit luminescence, the intensity of which is dependent on glucose concentration levels [1].

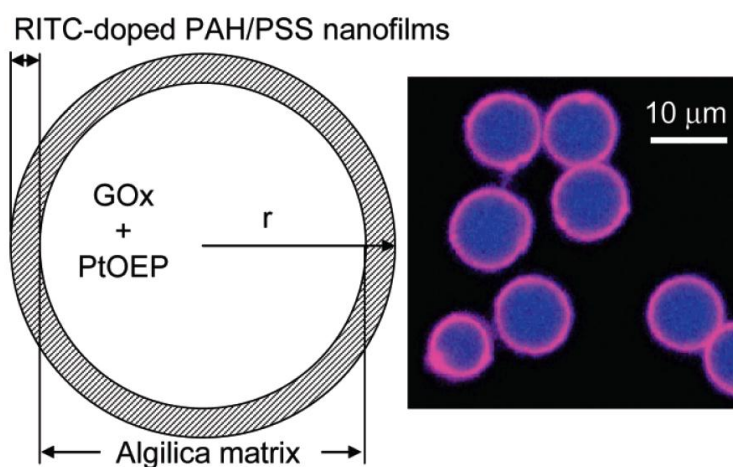


**Fig. 1** Schematic of enzymatic microparticle sensor and accompanying confocal micrograph depicting indicator (PtOEP, blue) and reference (RITC, pink) dye location [2].

Exploiting the aforementioned enzymatic reaction, dynamic sensor responses to varying glucose concentration levels are monitored. The sensor characteristics that are evaluated include sensor stability, response time, reversibility, sensitivity, detection limit and analytical range from hypo- to hyperglycemic levels [1, 2]. Some of these sensor properties including analytical range and sensitivity are modulated by varying parameters such as thickness and type of nanofilm coatings and method of nanofilm

deposition [2]. Other sensor characteristics depend on factors such as enzyme and oxygen concentrations, type of luminophores, and type of sensor matrix.

### Sensor testing apparatus

Fig. 2 shows a schematic of a custom dynamic testing apparatus that was developed to determine real-time changes in sensor response [1]. The dashed line in red includes the apparatus of particular interest in this project. While the basic setup and its purpose remains the same, some upgrades in the instruments highlighted in dashed line have been made.

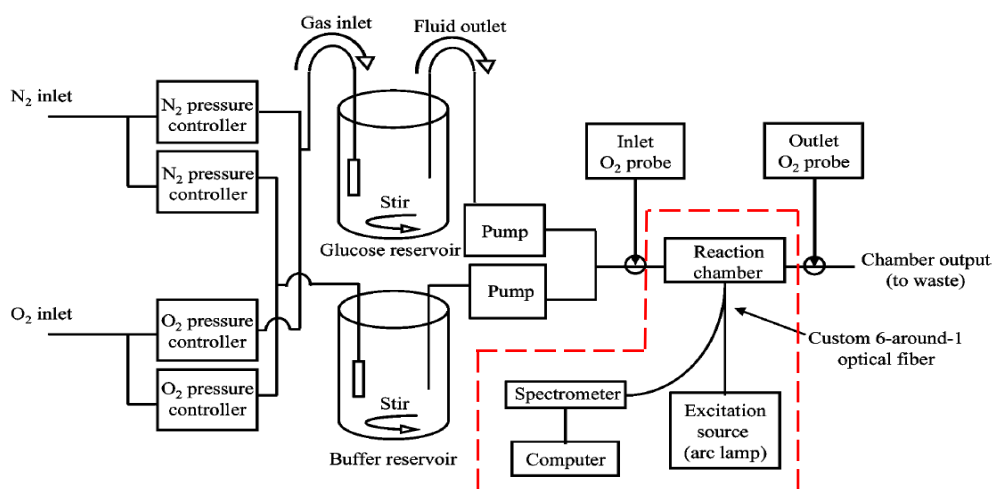


**Fig. 2** Schematic of dynamic testing apparatus used to quantify sensor response properties [1].

The excitation source and spectrometer have been combined into a single measuring tool called a Multi Frequency Phase Fluorometer (MFPF) manufactured by Tau Theta Instruments LLC shown in Fig. 3. This device contains an avalanche photodiode which

detects luminescence and an LED which serves as an excitation source for measuring optical biosensors' luminescent lifetime, intensity and phase shift [3]. A custom-designed bifurcated optical fiber bundle that is made up of several multimode fibers for collection and delivery is also employed.



**Fig. 3** A single channel MFPF manufactured by Tau Theta with Ocean Optics bifurcated optical fiber [3].

The reaction chamber contains a slot to hold a microscope slide on which an optical biosensor sample is immobilized. It also contains a port to which a bifurcated optical fiber bundle can be attached and interfaced directly with the sample. Green light from the LED can excite the sample and cause it to emit luminescence (Fig. 4). The amount of luminescence from the sample depends on the ambient oxygen concentration. Some of the luminescence entering the optical fiber travels back to the MFPF and is collected by the photodiode detector. The luminescence is analyzed in the Tau Theta software and then sent to the LabVIEW software to be recorded along with glucose concentration.

Most sensor characteristics such as sensitivity, optimal range and response time are determined by the luminescence response analyzed using this method.

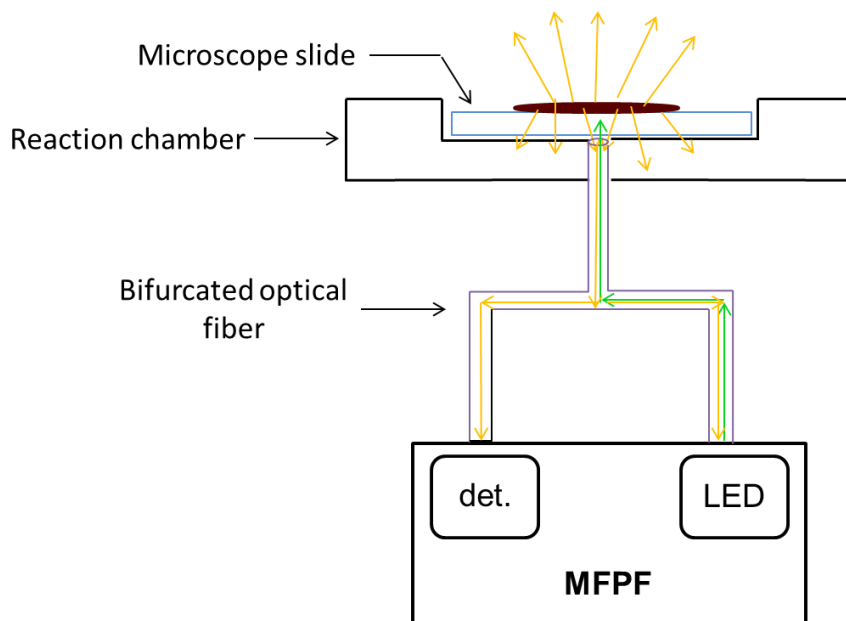


**Fig. 4** A portion of dynamic sensor testing apparatus containing the MFPF, optical fiber and the reaction chamber. Green light from LED is used to excite the sensor sample that emits orange light. Some of the emitted light enters the optical fiber and is measured by the detector (det.).

### Research motivation

As demonstrated in the previous section, the sensor response properties are currently determined *in vitro*. Before *in vivo* testing can be performed, complete sensor characterization must be determined. Research has shown that varying a sensor parameter, such as the nanofilm type or thickness, results in a different sensor response characteristic such as analytical range [2]. This implies that to determine an optimal

sensor characteristic, a significant number of characterization tests must be performed. Moreover, a single characterization experiment typically takes more than twelve hours which is a significant amount of time considering the number of experiments that need to be performed. Finally, micrometer scaled optical biosensors targeting other biochemical analytes will also be developed in the future, requiring further sensor testing. These limitations of sensor testing sets up a motivation to find ways that will accelerate the sensor development process. In this research project, several ways to achieve this goal are explored.

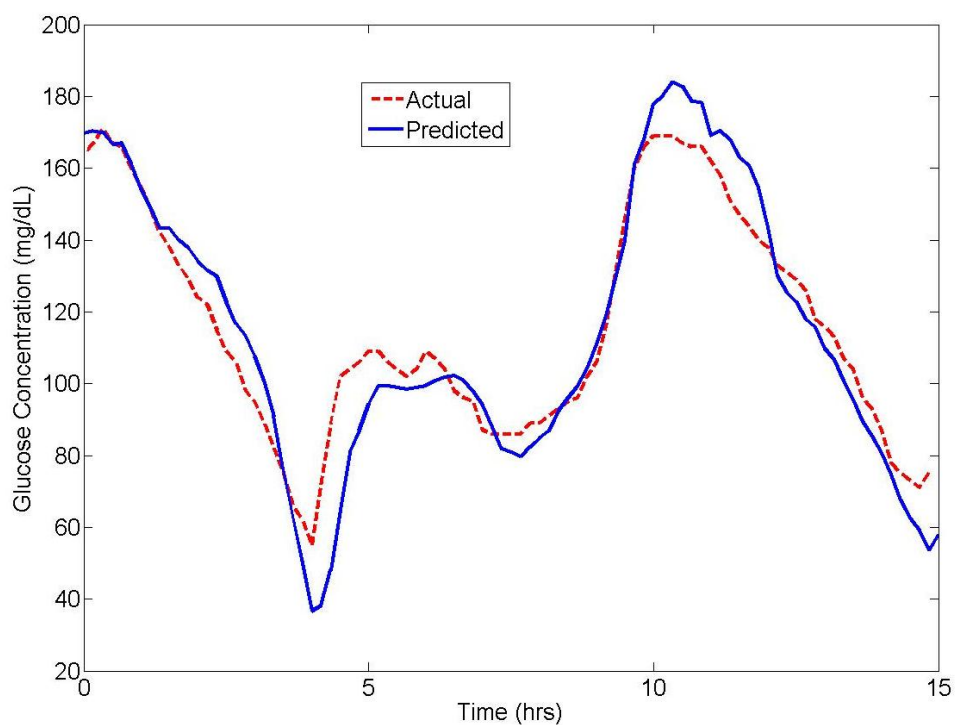


**Fig. 5** Comparison of the actual glucose concentrations exposed to the sensors and the predicted glucose level based on the sensor response. This graph demonstrates one example of sensor data that took about 15 hours [6].



Fig. 5 demonstrates an example of one type of characteristic tests conducted on sensor samples. It shows that this particular experiment took about fifteen hours for substantial data to be collected. The glucose concentration profile is similar to one seen in a patient with Type II diabetes. The graph shows the actual glucose concentrations exposed to the sensors and the predicted glucose level based on the response of the sensor. A lot of similar tests need to be conducted before *in vivo* testing can be performed which gives an idea of the amount of time for sensor development process [6].

One factor that contributes to long experimentation time is the low diffusion coefficient of the sensor matrix. This means that reactions take time to reach steady state and since the measurements are taken only when the sensor reactions reach steady state, the experiments are long. Another factor is that each sensor characterization test is performed at eight to twelve different analyte concentrations for comparison and steady state must be attained at each concentration level before measurements can be made. Since these factors are inevitable in experimentation, they cannot be exploited for faster sensor development. However, I believe that multiple sensor characterization tests can be performed at a time which will accelerate the development process, which is the main focus of this study.

### **Options for multiple sensor testing**

One way to test multiple sensor samples at a time is to use multiple measurement tools – the MFPPs. The only change to the experimental setup shown in Fig. 2 will be inside the

dashed box. Each reaction chamber contains up to three fiber ports hence three sensors can be placed in one reaction chamber. Bifurcated optical fiber from each MFPPF can be attached to each of the ports in a reaction chamber. However, this method employs purchasing a set of measuring tools and optical fibers for each sensor sample. Since, one channel MFPPF costs \$5,000 from Tau Theta Instruments and each optical fiber costs more than \$500 depending on its construction, other cost-effective solutions that can allow multiple sensor testing with only one MFPPF and optical fiber were explored.

### **Project objective**

The objective of this research project was to accelerate the sensor development process by allowing multiple sensors to be characterized at a time using a single measuring device, the MFPPF. For this purpose, an optical multiplexer (MUX) device was developed that enabled multiple sensor testing using only one MFPPF. Although, it did not reduce the time of each experiment, it allowed multiple experiments to be performed simultaneously. This eliminated the need to purchase a new set of measurement devices for each sensor test to be performed concurrently. Moreover, it simplified direct comparison between sensor samples without making corrections for variation in instruments while using multiple MFPPFs. Therefore, the MUX reduced the overall cost and time required for characterization experiments while increasing the overall data throughput without loss of performance. This unique design of optical multiplexer will lead to faster development of the biosensors and in turn allow earlier *in vivo* testing, possibly leading to valuable medical product in the future.

## CHAPTER II

### MATERIALS AND METHODS

This chapter explores the purpose of the optical MUX and different design concepts in which it can be constructed. The final MUX design that was chosen based on cost, efficiency, optical attenuation losses, and scalability is described with required individual components and their functions. Finally, methods used to perform experiments to evaluate the performance of MUX are described.

#### **Multiplexing and demultiplexing**

Multiplexing is a process in which information bearing signal from one input source is transmitted selectively to multiple output destinations [4]. Demultiplexing is the reverse of multiplexing in which information-signals from multiple output sources are selectively transferred to a single input source. A multiplexer is a device that allows multiplexing and similarly, a demultiplexer is a device that performs demultiplexing.

The optical multiplexer (MUX) device developed in this research project employs both multiplexing and demultiplexing processes. The signal transmitted in MUX from a single input channel (the MFPP) to multiple output channels (the sensors) and *vice versa* is light. Fig. 6 demonstrates these two concepts employed in the optical MUX. In the forward direction, the MUX acts a multiplexer transmitting green light from the LED inside the MFPP to the biosensor samples for their excitation. In the reverse direction,

the MUX acts as a demultiplexer transferring luminescence from the optical biosensors to the detector in the MFPP. The MFPP is attached to MUX through an input fiber – the bifurcated multimode optical fiber that carries light in both directions. The MUX is attached to  $n$  number of samples in the reaction chambers via  $n$  output fibers – the multimode optical fibers.

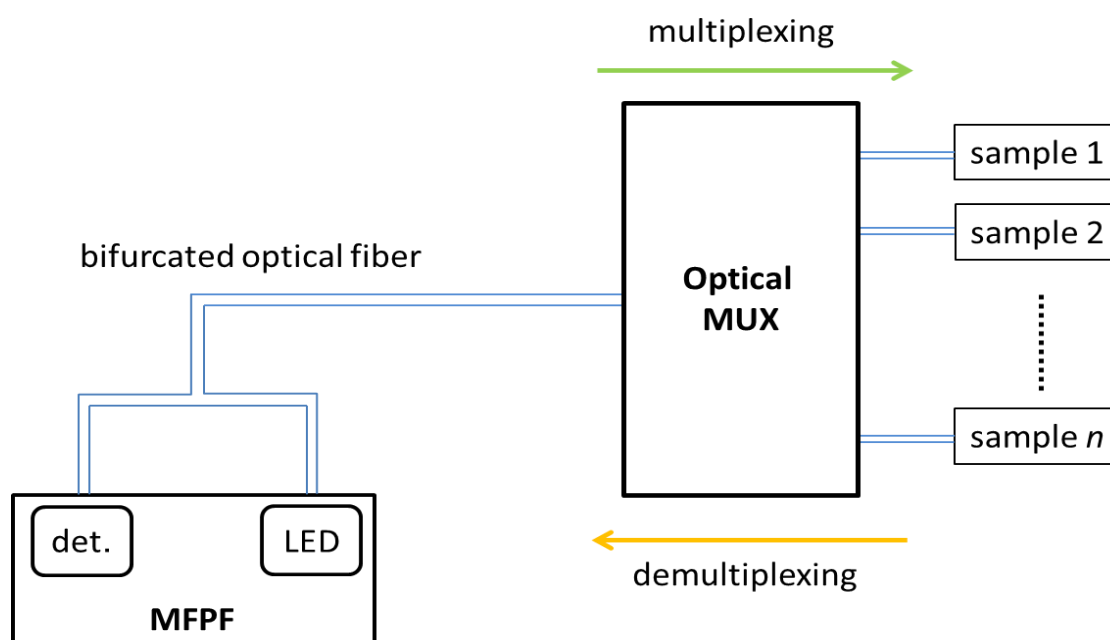


**Fig. 6** Multiplexing and demultiplexing by the optical MUX. Forward green arrow shows multiplexing from MFPP to  $n$  number of samples and reverse orange arrow shows demultiplexing from  $n$  samples to MFPP. The blue lines indicate multimode optical fibers that carry light in either direction.

### Functionality of optical MUX

As demonstrated, the main purpose of optical MUX is to allow simultaneous testing of multiple biosensor samples using a single measuring tool (MFPP) and bifurcated optical fiber. The rectangular box representing optical MUX in Fig. 6 consists of two main

sections—the Motion Control Unit and the Optics Section. The main purpose of each section is described below. The final MUX prototype developed in this research project was constructed with three sample channels for simplicity and limited budget. Three channels were sufficient to prove the concept of MUX. However, the final MUX design was flexible such that it could be easily scaled up to more than three channels.

#### *Motion control unit*

The MUX transmits input light through the optical fibers to the samples (and collects output light from the samples) one-by-one at each sample position. This means that it switches input light between the samples while temporarily disconnecting it at each sample position. In the original experimental setup discussed in Fig. 4, the light from LED is exposed to the sample periodically to prevent damage from overexposure to the sensors. Since the input light does not have to be continuously exposed to the sample and the luminescence need not be continuously collected for measurements, multiplexing and subsequent demultiplexing by the optical MUX can be performed. Light from the input optical fiber can only be switched between the sensor samples when the input fiber is physically moved from one position to the next. This physical switching of input fiber from MFPF to each sample position was achieved by the Motion Control Unit.

### *The optics section*

While the Motion Control Unit moves the input fiber from the MFPP, it transfers light from LED to the three output fibers attached to the reaction chamber containing the sensor samples. Since the input fiber has to physically switch between the output fibers, it is not directly interfaced with the output fiber when light is being transferred between them. Instead these fibers are placed at a distance with an air gap in between. As the light travels through the air gap, it spreads out i.e. it diverges. Only a portion of this input light enters the output fiber since the light intensity decreases with increasing distance (Fig. 7). The Optics Section containing several optical elements was used to minimize this divergence of light in air and effectively transfer it between the input and output fiber and *vice versa*.

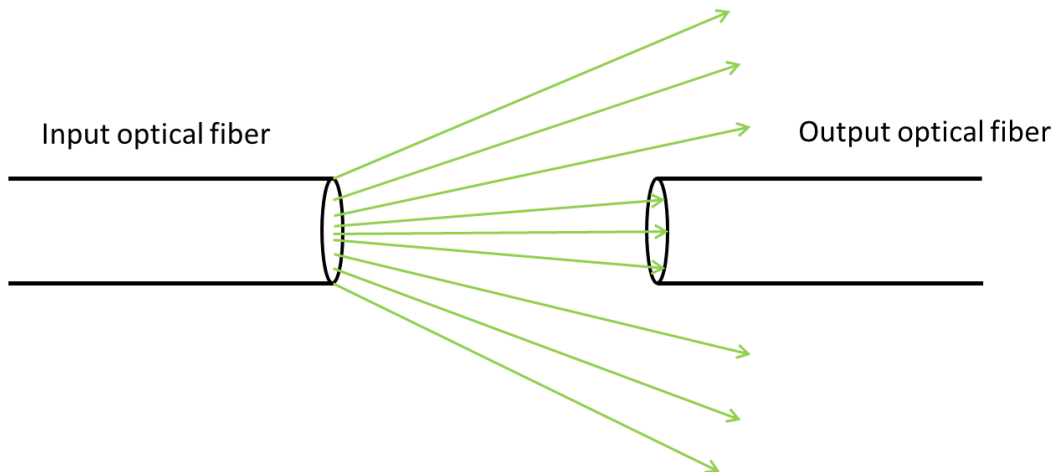


**Fig. 7** Divergence of light as it leaves the input optical fiber. Only some of this light is captured by the output fiber placed at a distance.

### **Selection of the two MUX parts**

After describing the main purpose and concept of each MUX part, different types of components and design concepts that could be used to make these parts of MUX are separately discussed in this section. The most effective components and design concepts in terms of cost, efficiency, optical data losses and scalability were chosen for final development of the MUX.

#### *Selection of optical elements for the optics section*

Diverging light from the optical fiber can be focused into a straight parallel path *i.e.* collimated, by using a collimator [5]. Two types of collimators that can be used for this application are plano-convex lenses or aspherical lenses. Both types of lenses are flat on one side and curved (convex) on the other for collimating diverging light or focusing a collimated light. Aspherical lenses are different from plano-convex lenses in their curved surface profile. The convex part of aspherical lens is designed to eliminate optical aberrations such spherical aberration, which is an optical loss arising from curved surfaces [5]. Plano-convex lenses also reduce spherical aberration but do not entirely eliminate it. Due to this, aspherical lenses are typically three to four times more expensive than plano-convex lenses. For Optics Section, plano-convex lenses were chosen since they were more cost-effective. However, to reduce reflective losses from the surface of the lens, plano-convex lenses with an anti-reflective coating were chosen.

The process of collimation by plano-convex lenses between the optical fibers is shown in Fig. 8. Note that two lenses are used between the fibers – first to collimate the diverging light and then to focus collimated light in to the fiber. The lenses are placed at a distance of one focal length,  $f$ , from the fiber to focus light into the fibers. Note also that only green light from the input fiber attached to the LED is shown. In reality, luminescence from output fiber attached to the sensor samples also travels in the reverse direction to that shown in Fig. 8.

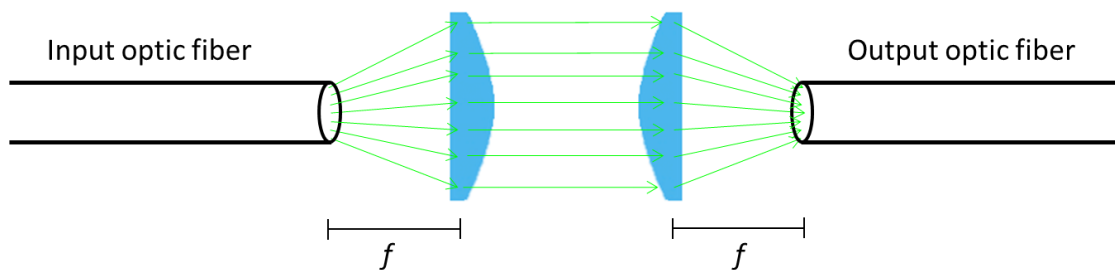


**Fig. 8** Efficient transfer of light by plano-convex lenses from input to the output fiber. The lenses are placed at a distance of one focal length of the lens which is denoted by 'f'. Only green light from the input to the output fiber is shown.

Once the type of lens was chosen, the next task was to select the size and appropriate focal length of the lens. The choice of lens size depends on the numerical aperture of the optical fiber used. Numerical aperture is an optical perimeter that measures an optical element's acceptance angle of light [7]. In order for light to be completely directed onto an optical element (the fiber or lens in this case), it must fall within this angle (Fig. 9). Therefore, for light from the optical fiber to fall within the size of lens, the numerical aperture of the lens should be equal to or lower than that of the fiber. If the angle is



larger, then some of the light will escape from above and below the lens lowering the efficiency of system (Fig. 9).

The lens cannot be placed closer than the focal length of the lens to capture all of the light. It has to be placed at the focal length in order for luminescence coming from the other end to be focused into the fiber. The numerical aperture of the optical fibers used is 0.22 and the lens chosen for this application has a numerical aperture 0.42, which is well above the required value to ensure higher efficiency.

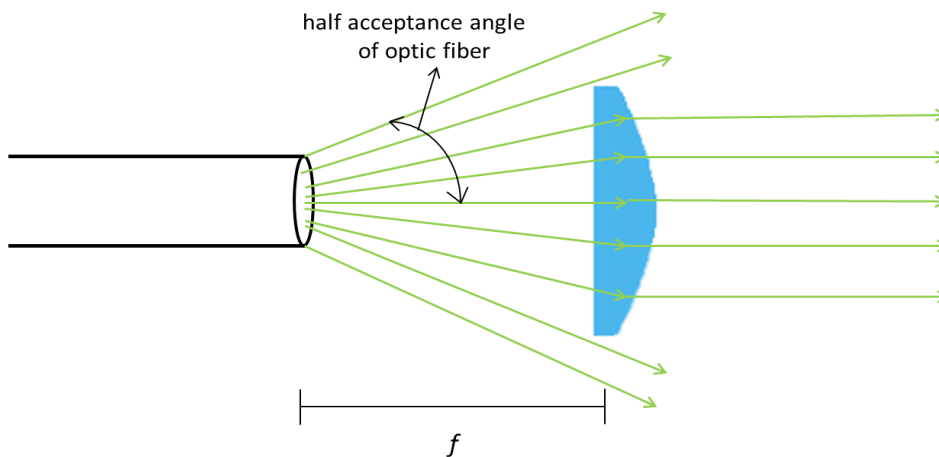


**Fig. 9** Efficient transfer of light by a lens between input and output fiber. Half acceptance angle of fiber is greater than that of the lens. The lenses are placed at the focal length of the lens which is denoted by 'f'.

Other optical elements needed for the MUX mainly served the purpose of holding and mounting the lens and the optical fiber together. Table 1 provides a list of all the optical elements, purchased from ThorLabs, with their description of dimensions, quantity and

function. Fig. 10 shows all of the optical elements integrated together to form one channel of the Optics Section. It also demonstrates how light travels within a channel of the MUX. An optical fiber from the LED was attached to the lens tube via SMA fiber adaptor plate. The lens was placed inside the lens tube and fixed to a desired position using retainer rings. The lens tube was held on an optical post through fixed mounts. These mounts were screwed into steel posts that were attached to an optical breadboard for testing.

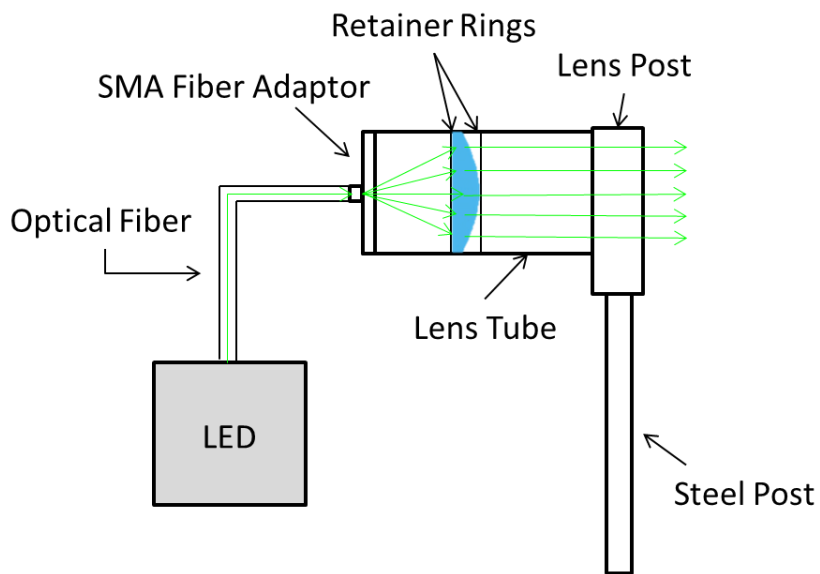


**Fig. 10** All optical elements integrated together to form one channel of the Optics Section. Green light from the LED travels through an optical fiber connected to lens tube via SMA fiber adaptor and diffuses in the lens tube. Within the lens tube a plano-convex lens is placed which collimates and transmits light to the lens post. This particular channel is the input channel since it is connected to an LED inside the MFPF (not shown).

**Table 1** Optical elements for the Optics Section.

<b>Optical Element</b>	<b>Part Number</b>	<b>Dimensions and Quantity</b>	<b>Function</b>
Plano-convex lenses with antireflective coating	LA1504A	$f = 15\text{mm}$ , $d = 0.5\text{ inch}$ , 4 pieces	Collimation of light
Lens Tubes	SM05L10	$l = 1\text{ inch}$ , $d = 0.5\text{ inch}$ , 4 pieces	Holding lens
SMA Fiber Adaptor Plate	SM05SMA	$d = 0.535\text{ inch}$ , 40 threads, 4 pieces	Connecting optical fiber to the lens tube
Retainer rings		12 pieces	Fixing and positioning lenses inside the lens tube.
Spanner Wrench	SPW603	1 piece	Adjusting retainer rings
Stainless Steel Optical Posts		$d = 0.5\text{ inch}$ , 4 pieces	Mounting lens tube to the optical bread board
Compatible Fixed Mounts	SM05	4 pieces	Mounting lens tube to the optical posts
Motey optical adjustment tools for post and mounting		4 pieces	To allow positioning of optical posts on optical bread board
Optical Breadboard		1 piece	Hold all fibers and provide platform for testing

$f$ = focal length;  $d$ =diameter;  $l$ =length

### *Selection of motion control unit*

Once the optical components were finalized, the next task was to research design options and devices for the Motion Control Unit that would mount the input optical fiber bundle and allow it to switch between multiple channels (at least three for the MUX prototype).

Both commercially available and personally designed systems with actuating components were explored. Following factors were considered before selecting final product for the Motion Control Unit. The actuating system should be:

1. able to provide either rotational or linear motion by some type of motor,
2. able to provide precise positioning,
3. cost effective (less than a thousand dollars),
4. capable of being extended to more than three channels,
5. able to mount an optical fiber,
6. able to be constructed within two months.

All of the considered options included a motor, a motor driver and a motor controller. A motor is a device that provides an actuating motion; a motor driver provides appropriate signal to drive the motor; and a motor controller that can be based on either software or hardware controls the motor operation, direction and speed.

### *Linear actuators*

A linear actuator is a tool that creates linear motion of a device mounted to it. The best option for this project was to use an electro-mechanical linear actuator. One option was to use a motorized linear actuator or a slide with a controller. Several products from

various companies were explored. Zaber Technologies provides many products to select from, for example the motorized linear slides with built-in controllers. This device provides automatic control through software with very high precision; however, it was too sophisticated for this application and was above the allocated budget.

Another option was to build a linear actuator using a motor and a lead screw attached to the motor shaft. The input optical fiber could be attached to a lead screw. The motor would rotate the lead screw which would allow linear displacement of the fiber (Fig. 11). This concept, although simple, was complicated to implement since it required a sensor and feedback mechanism to detect the position of the fiber on the lead screw. This method would not provide the precision required for this project's application.

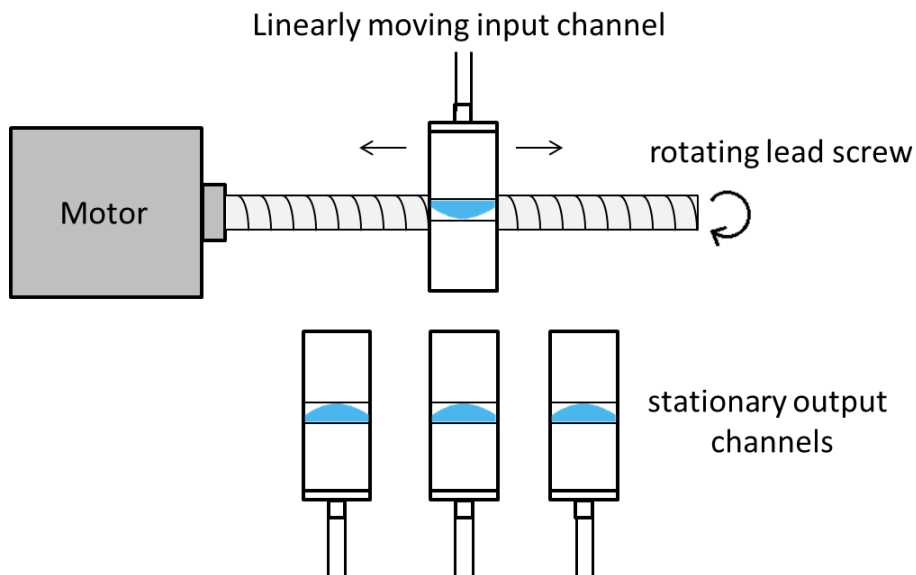


**Fig. 11** Linear actuator built from a lead screw attached to a motor. This device would allow linear displacement of input fiber as the lead screw rotated.

### *Rotational devices*

A rotational device provides rotational motion of an object mounted to it vertically.

Several commercially available motorized rotational stages with built-in controllers were explored. However, due to their high cost, this option was also dropped.

A cheaper alternative was to build a custom made rotational device. One such device was theoretically created based on a reduction gear method. A metal steel plate, to which the input fiber can be attached, would be connected to a motor using two metal rods (Fig. 12). As the motor would run, the steel plate would rotate causing the fiber to rotate with it. The output fibers would be attached to another steel plate mounted on a wall facing the first steel plate. This concept was not pursued due to its complexity in mounting steel plates to a motor and to a wall. Another disadvantage of this design was that the input fiber would rotate continuously in one direction if more than three channels are desired, causing twisting or macro-bending of the fiber which is not feasible for optical transmission of light. Moreover, a motor controller with feedback mechanism would also be required.

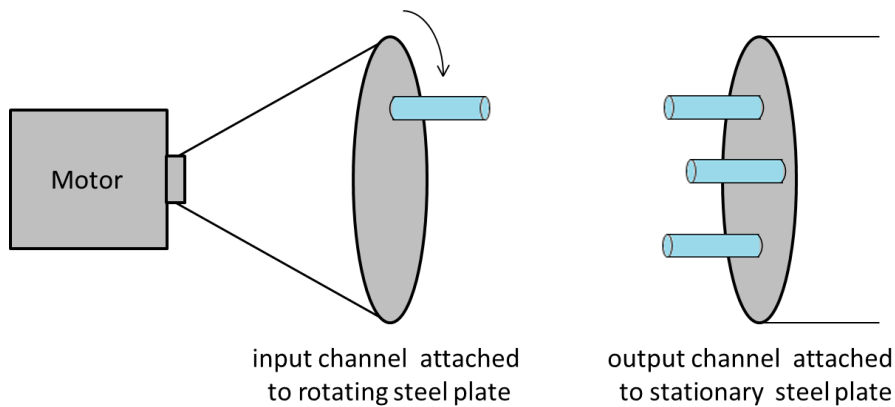


**Fig. 12** Concept of a rotational device based on reduction gear method.

A different option for providing light to several output fibers from the input fiber was also explored. Instead of mounting the input fiber onto a motor, a mirror would be mounted to it and placed between the input and the output fibers. This mirror would rotate in one plane and reflect light sequentially at different directions to the positions where the output fibers would be mounted (Fig. 13).

This design was considered since it did not require any movement of the input fiber, hence eliminating macro bending losses in the fiber. However, the mirror would introduce inherent reflection and transmission losses that would be difficult to reduce. Also, mounting the mirror on the motor such that it provided movement in one plane would be difficult and mounting the output fibers around the mirror would require an additional mounting frame.

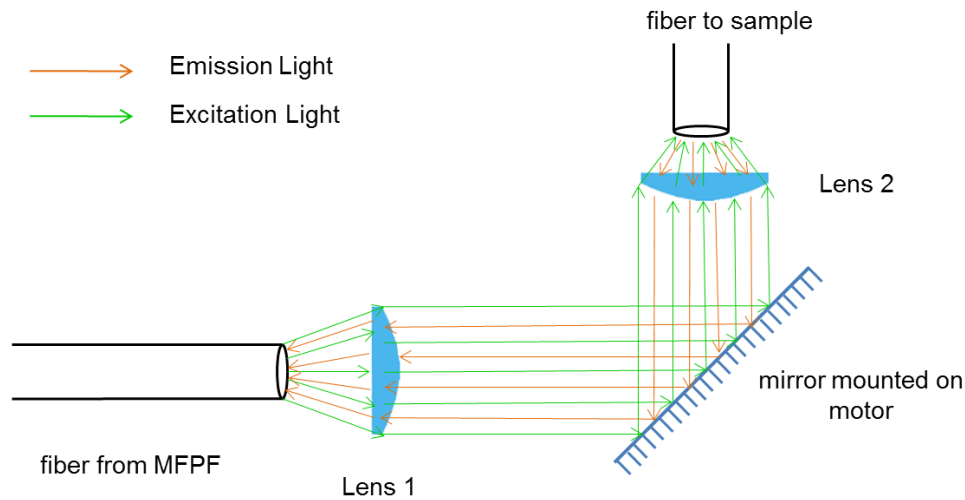


**Fig. 13** Transfer of light between the fibers through reflection of a mirror. Orange light is emitted luminescence from a sample collected into the fiber and green light is excitation light coming from the LED inside the MFPF.

#### *Final design of motion control unit*

The most appropriate solution that was chosen included a stepper motor, a simple driver circuit and software based motor controller. The motor rotated the input fiber in the horizontal (consider x-y axis) plane. The output fibers were placed around the motor in the horizontal plane at fixed positions and at equal angular displacements.

A stepper motor was chosen instead of a DC motor because it provides more precise positioning than a DC motor. A stepper motor divides one full rotation into several steps, each equaling a certain number of degrees of rotation. Unlike a DC motor which can take any position in one rotation, a stepper motor can only rotate within these steps without requiring any feedback mechanism. The stepper motor, therefore, allows reliable start and stop motion at desired positions. The motor purchased for this project was



12VDC Unipolar Stepper Motor (Manufacturer no. 42BYGH404-R) from Jameco Electronics. One step rotation of this stepper motor is equal to 1.8 degrees. To mount the fiber to the stepper motor shaft, an aluminum mounting hub with custom made screw holes was used.

With the hardware driver circuit and software based controller, a DAQ (data acquisition) hardware was required to process the signals from driver circuit to the computer. While exploring efficient yet inexpensive options, a USB DAQ training kit from EMANT Pte Ltd. was found. This kit includes EMANT300 USB DAQ module with an associated 24V DIO (digital input/output) application adaptor and a motor controller program in LabVIEW software. The application adaptor has a built-in stepper motor driver chip, ULN2003, and can be directly interfaced with computer using USB DAQ module. The motor controller program can be modified to control the motion of the stepper motor as desired. This solution was under the allocated budget and provided a solution that can be implemented with relative ease. Fig. 14 shows all the components integrated together to form the Motion Control Unit of the MUX.

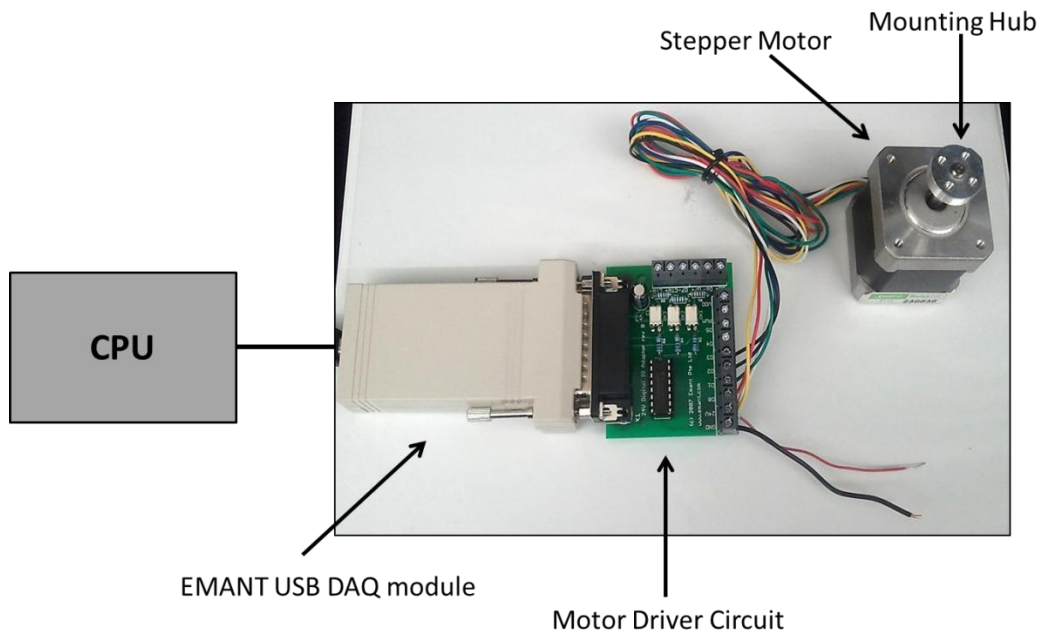


**Fig. 14** The final configuration of Motor Control Unit. It contains a stepper motor to which fiber mounting hub is attached. The motor is connected to motor driver circuit which is attached to the USB DAQ module. The DAQ module connects the driver circuit to a computer via USB port.

### **Final configuration of optical MUX**

Fig. 15 shows a schematic of the Optical Section and Motion Control Unit integrated together to make up an optical MUX. The following description of the motor controller program in LabVIEW demonstrates how the MUX system works. This design is flexible such that it can be easily extended to more than three channels by simply adding more output channels and placing them around the motor. Angular displacement (the number of motor steps) and steady state time (the time motor is stationary at a channel) can also be altered in the LabVIEW controller program to accommodate additional channels.

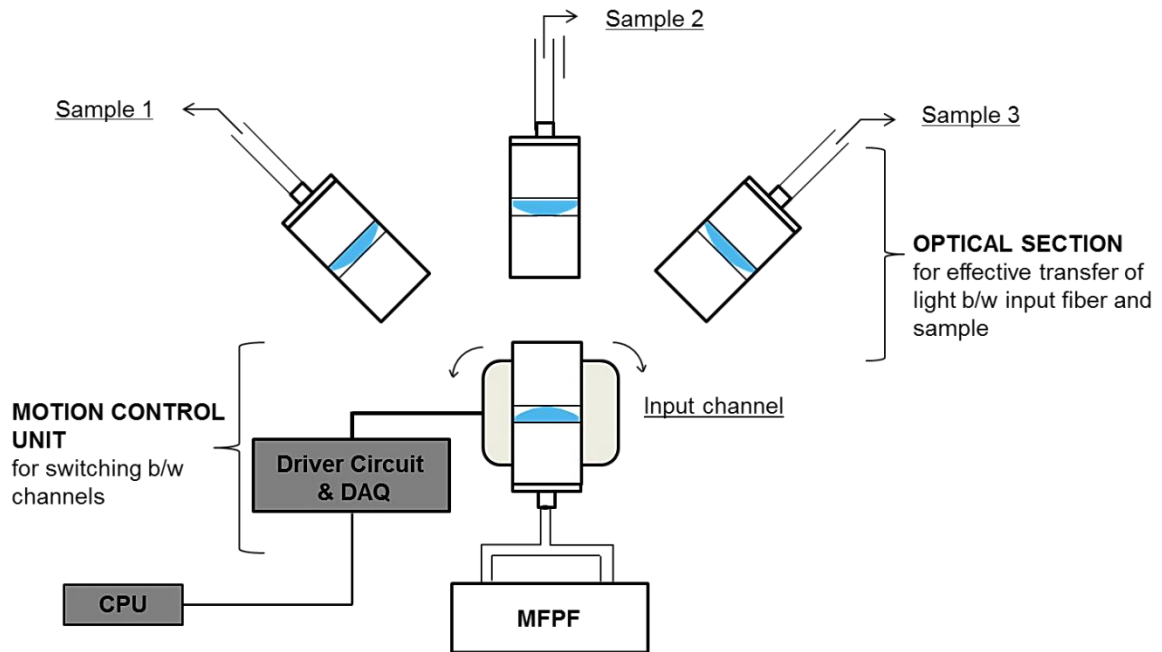


**Fig. 15** Schematic of Optical Section and Motion Control Unit integrated together to make up an optical MUX.

### *LabVIEW motor controller*

The LabVIEW motor controller program from EMANT was modified to allow repeatable motion of the input channel to three fixed locations of output channels placed 45 degrees apart (Fig. 15). At first, the motor is positioned to face output channel connected to sample 1. When the program is started, the input fiber mounted to the stepper motor shaft rotates 25 steps clockwise with angular displacement of 45 degrees (1 step = 1.8 degrees) and stops for three seconds at sample 2 position. It then takes another 25 steps to reach sample 3 from sample 2 and stops for another three seconds. Then the motor reverses direction and rotates counter clockwise 50 steps to reach sample 1 position. This motion is repeated until the program is stopped.

### **Methods for testing the MUX performance**

Once the MUX was built, the next task was to find the overall performance of the MUX system. It was expected that the light travelling through the MUX would be attenuated and the optical efficiency might be reduced. There are many reasons for optical losses which accumulate to make up total attenuation loss [7]. Some of these reasons are listed below.

1. The losses in an optical fiber occur due to imperfect light coupling at the ends of a fiber and absorption and scattering within a fiber that increase with the number and length of fibers. Micro-bending (tiny kinks or ripples that form in the fiber length caused by deformation of fiber) and macro-bending (physical bending of the fiber visible to an eye) are other sources of light leakage in a fiber [7].
2. Absorption and reflection losses within and at the lens surface can also occur. Although, these losses should be minimum as plano-convex lenses with antireflective coating are used.
3. Attenuation due to absorption of light by air can occur as the travel distance of light in air is increased. This should not add up to be a significant loss since air does not absorb much of visible light. Scattering or divergence of light as discussed before is another attenuation factor by air.
4. Light will also be lost if the optical channels are not perfectly aligned and if the lenses are not placed at the focal length.

To determine the effect of these attenuation factors on the performance of the MUX, several tests were performed. These tests determined the overall efficiency of the MUX,

collimation of light in air gap between the fibers and the effect of a moving fiber on the intensity of light. Only one set of optical channels was chosen for all tests since all channels were made up of identical optical elements and would give similar results. The following measuring devices and equipment were used for the following experiments:

1. USB4000 Miniature Fiber Optic Spectrometer from Ocean Optics
2. LLS-470 Ergonomic LED light source (Visible) from Ocean Optics
3. OOIChem Spectrometer Operating Software (Oceans Optics, Inc.)

#### *Determining reference value*

A fixed value of light intensity, called the reference value, was measured and then passed through an optical channel of the MUX to determine the reduction in that value which was called the MUX value. A light intensity from variable LED was adjusted and measured by using USB4000 spectrometer connected to the LED through an optical fiber (Fig. 16). The spectrometer was connected to a computer via a USB port and the light intensity was measured at one wavelength in the spectrometer operating software. The light intensity was measured in number of counts which is a unit proportional to the number of light photons collected.

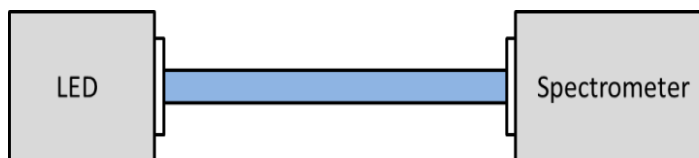


**Fig. 16** Setup for measuring reference value. LED is directly connected to the spectrometer using an optical fiber. The spectrometer is connected to a computer.

### *Setting up the software*

Certain sampling parameters in the software were adjusted before measurements were taken. The most important task was to ensure that the spectrometer did not saturate. The spectrometer used in the experiments has a saturation limit of 65000 counts, which is the maximum intensity it can measure. The reference intensity value from the LED was chosen such that it was less than the saturation limit of the spectrometer.

The integration time is the amount of time a spectrometer captures lights. The longer the integration time the greater is the number of counts measured. It was adjusted such that maximum signal intensity was measured without saturating the spectrometer. A background signal, called the dark spectrum, resulting from the ambient environment was also measured and subtracted from the data signal. This was done in order to receive a pure data signal without background noise. Finally, averaging function called, the boxcar, was applied to average a few intensity values in order to reduce the fluctuations in light intensity. The values of these parameters will be mentioned in the next chapter on Results.

### *Experimental setup for tests*

After setting up the reference intensity, light intensity through a MUX channel was measured. This was called the MUX value. Fig. 17 shows this experimental setup. The optical fiber from the LED was attached to the input channel and the fiber from output channel was attached to the spectrometer. Light from the LED passed through the input

and output channels and entered the spectrometer that measured the light intensity. Both input and output channels were aligned so that they were at the same height directly facing one another to prevent positioning losses. This experimental set up was used in the Efficiency test and the Distance test discussed in Results chapter. The optical efficiency was calculated using equation (1).

$$\% \text{ efficiency} = \frac{\text{MUX value}}{\text{Reference value}} * 100 \quad (1)$$

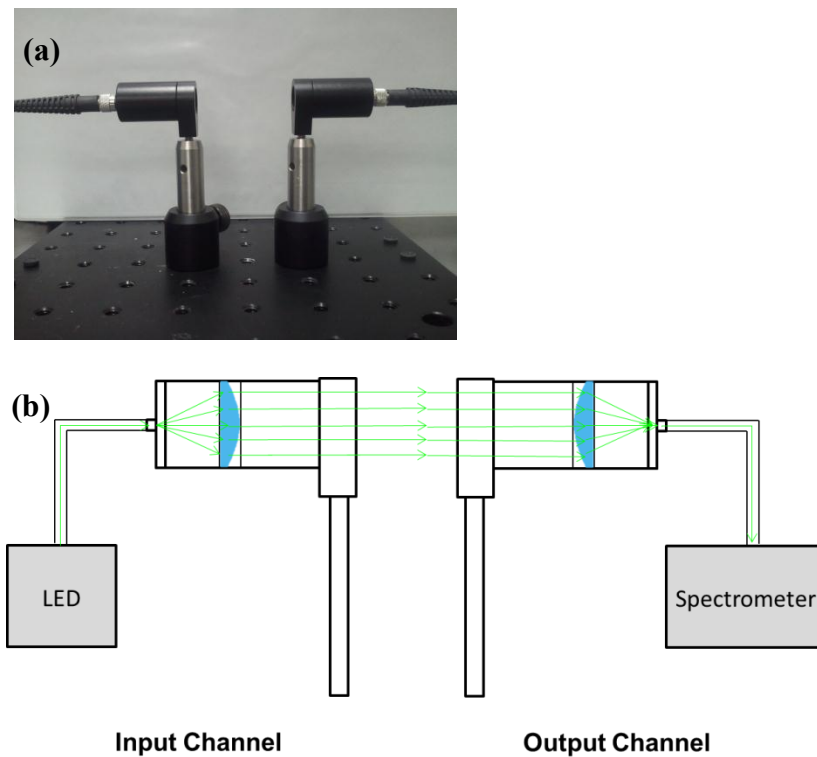


**Fig. 17** Experimental setup for measuring light through one of the MUX channels. (a) Picture of the setup showing input and output channels mounted on an optical breadboard. (b) Schematic of the setup with the LED and the spectrometer.

### *Set up for motion control test*

This test is called the Motion Control test because it employed the Motion Control Unit. It was performed to determine the effect of a moving fiber on the light intensity measured by the spectrometer. The picture in Fig.18 shows the experimental setup used for this test. Only one of the output channels was connected to the spectrometer for testing. The fluctuation of light intensity was measured as the input fiber mounted on the stepper motor shaft switched between the output channels.

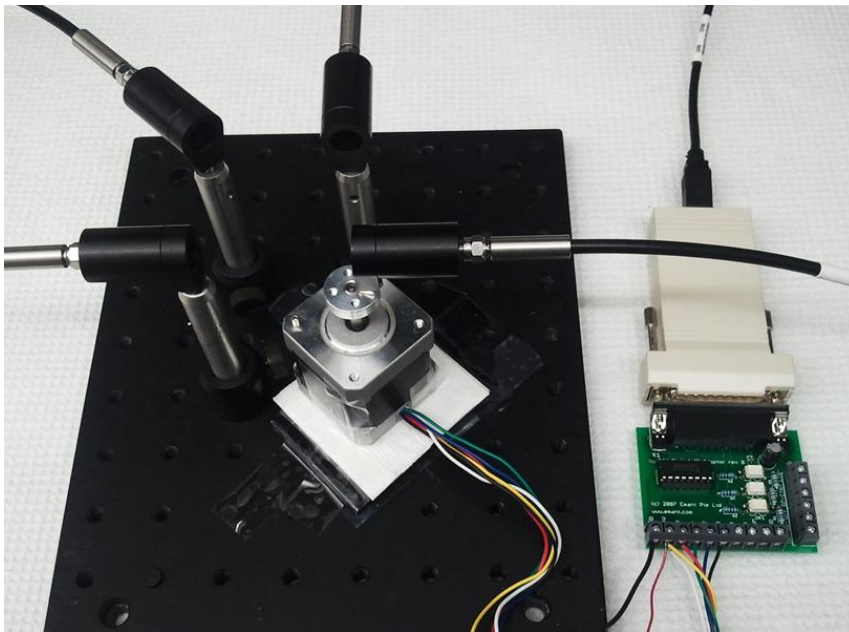


**Fig. 18** Experimental setup for the Motion Control test.



## CHAPTER III

### RESULTS

This chapter describes the purpose and results of the three experiments conducted on the optical MUX to determine its performance. The three tests were the Efficiency test, the Distance test and the Motion Control test.

#### **Efficiency test**

##### *Purpose*

To investigate the efficiency of the MUX, five sets of reference values were recorded with their respective MUX values. The spectrometer measured light intensity at a spectrum of wavelengths but the reference and MUX intensity values were determined at only one wavelength. Distance between the two channels was fixed when taking five data points. Sampling parameter values are shown in Table 2.

**Table 2.** Sampling variables for the Efficiency test

<b>Sampling Variable</b>	<b>Value</b>
Distance	2 inch
Wavelength	542.77nm
Integration Time	1 msec
Boxcar width	25

### Result

Fig. 19 shows a graph of light intensity of reference values and corresponding MUX values measured at five different data points. The efficiency at each data point was measured using equation (1) and is shown by the red line corresponding to the efficiency axis on the right. The average efficiency calculated for the MUX using these five data points was 54.3% with a standard deviation of 1.4. This means that almost half of the light was attenuated in the MUX channel. However, this is not a major problem for sensor data testing since the intensity of LED can always be increased to achieve the desired output intensity from the MUX. The standard deviation in these values was 1.4, which is a small variation in the efficiency showing that these data are very repeatable.

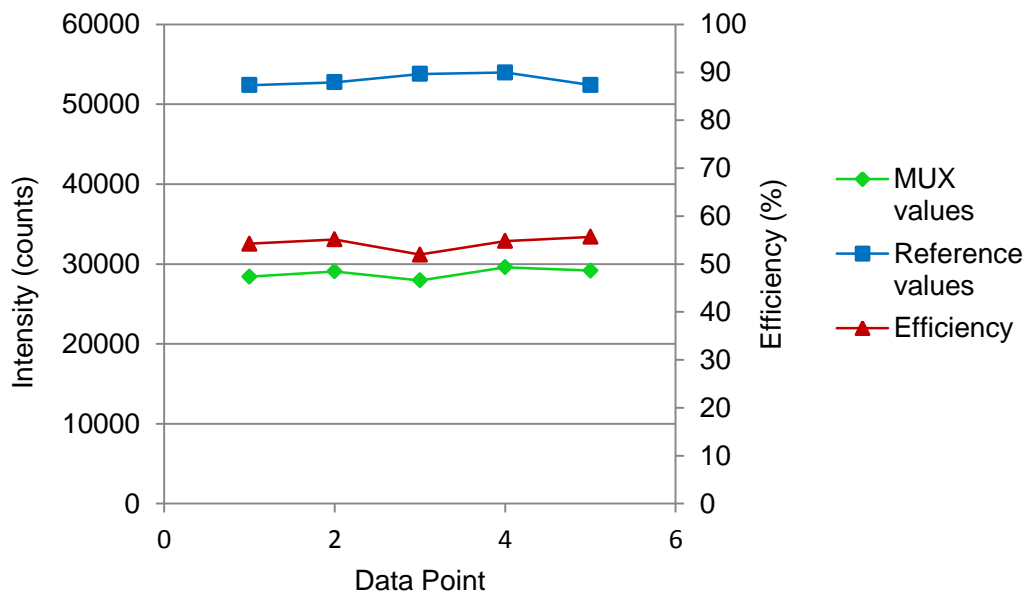


**Fig. 19** Graph of intensity (number of counts) and efficiency (%) at five data points.

## Distance test

### *Purpose*

This test was performed to determine the effect on collimation of light as a function of distance between the input and the output channel. As demonstrated in Fig. 20, the collimated light coming out of the input channel might diverge in air with increasing distance. The efficiency should go down as the distance is increased since some of the light would escape from around the lens tube at the opening of the output channel.

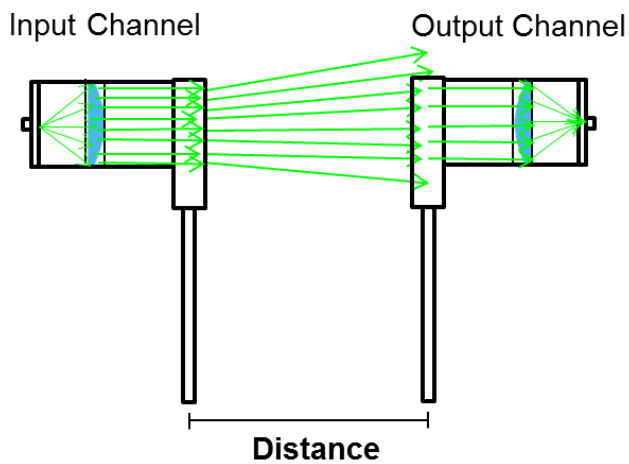


**Fig. 20** Divergence of light with increasing distance..

**Table 3.** Average efficiencies at three distances.

<b>Distance (inch)</b>	<b>Average Efficiency</b>
1	47.7% $\pm$ 1.2
2	54.3% $\pm$ 1.4
3	49.3 % $\pm$ 1.6

Average efficiencies were calculated from five data points at three different distances using the method employed in the Efficiency test. These values are shown in Table 3. Standard deviation at each efficiency value was obtained to show the variation in data.

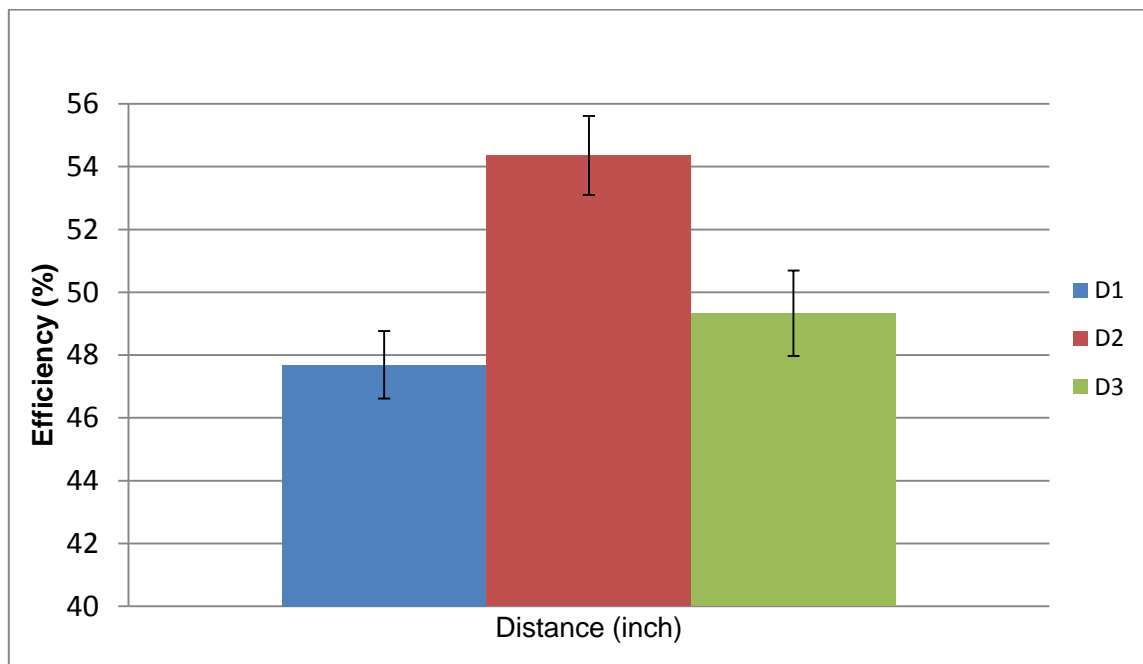


**Fig. 21** Bar chart of average efficiency at three distances between channels. D1, D2 and D3 bars represent distances at 1, 2 and 3 inches respectively. The error bars of 95% confidence intervals are also shown.

### *Result*

Fig. 21 shows that the average efficiency at distance 1 and 3 inches are  $47.7 \pm 1.2\%$  and  $49.3 \pm 1.6\%$  respectively, with the error bars of 95% confidence intervals overlapping.

At distance 2 inches the average efficiency is  $54.3 \pm 1.4\%$  which is higher than the former values with no overlapping of error bar. This variation in data is most likely caused by a systematic positioning error that resulted in decreased average efficiencies at

distance 1 and 3 inches. Since these data do not show a decreasing trend of average efficiencies with increasing distance and the efficiencies at distance 1 and 3 inches are comparable, it can be concluded that light was being collimated in the air gap. The results of this test signify that the three output channels need not be at the exact same distance from the input channel, because the effect of distance on light intensity is minimal to none. Therefore, slight distance variations among the channels would still result in comparable results for the sensors attached to the output channels.

### **Motion control test**

#### *Purpose*

This test was performed to determine the effect of moving fiber on the intensity of light measured by the spectrometer. While the input fiber mounted to the motor rotated between the channels, light intensity captured by one of the output channels was measured by the spectrometer. The intensity was measured as a function of time for a bandwidth of ten wavelengths (Fig. 22).

#### *Result*

The graph in Fig. 22 shows how light intensity as measured by the spectrometer varies with time. Twelve cycles of motor rotation are shown with a period of one cycle approximately equal to eight seconds. In each cycle, the length of a bar indicates the time when the input channel was at steady state and was facing the output channel connected to the spectrometer. The height of a bar indicates the light intensity. The red

arrow depicts the average intensity at each bar height which is roughly at 25500 counts for every cycle. However, a few spikes of intensity at the corners of bars are also seen that represent the transient state of the motor i.e. the time when the motor was just about to start or stop its motion.

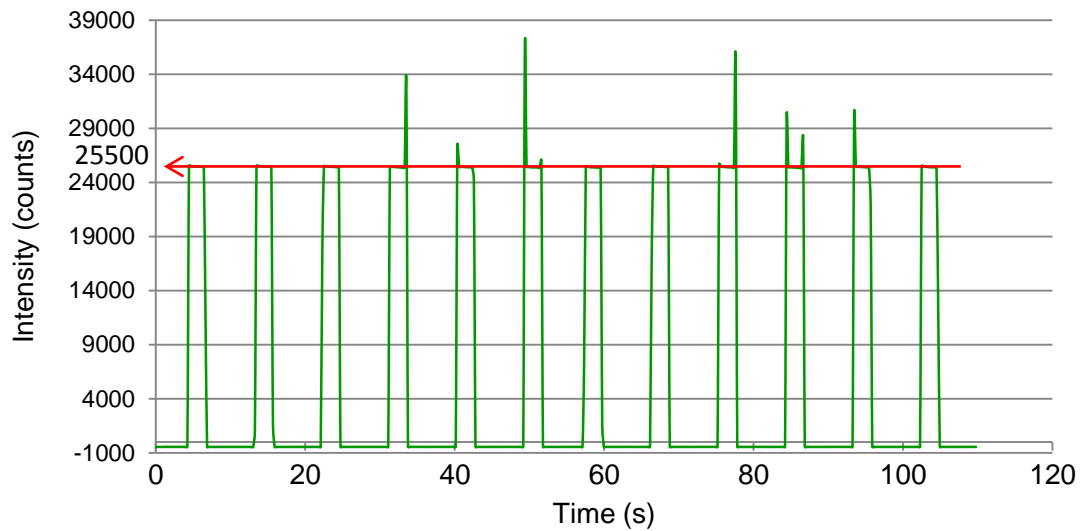


**Fig. 22** Graph of intensity versus time for the Motion Control test. It is measured at one of the output channels from the moving input fiber.

From these data, it can be concluded that intensity at a channel is constant over time at steady state with occasional intensity peaks occurring only at transient state of the motor.

To allow consistency in biosensor data, these peaks can be avoided by evaluating the data only at the steady state of the motor. The length of time for steady state can be changed in the software program to allow desired time for data collection.

## CHAPTER IV

### DISCUSSION AND CONCLUSION

#### **Benefits of MUX over MFPP**

The main purpose of developing an optical MUX, as demonstrated in this research project, was to allow multiple biosensors to be tested simultaneously using a single measurement tool – the MFPP. There are several benefits of using MUX over multiple MFPPs to achieve the same sensor data throughput. These advantages are discussed below.

The most significant advantage of using MUX is its lower cost. The total cost of a three-channel MUX is \$1,170. A one-channel MFPP costs around \$5,000. In order to achieve the same data throughput as with the three-channel MUX, two additional MFPPs would be required with total additional cost of \$10,000. A better comparison of cost can be demonstrated by comparing the price of adding one optical channel to MUX (which is \$400) versus cost of one MFPP (\$5,000) for testing an additional biosensor sample. This comparison reveals that the MUX is about twelve times more cost effective than the MFPPs. Moreover, increasing the number of channels will further increase the cost efficiency.

Another significant benefit of using MUX over multiple MFPPs is that it allows direct comparison of biosensors since only one MFPP containing a single detector and LED is

required. When using multiple MFPFs correction of variation among the detectors and LEDs is needed before the sensor data can be compared. Other advantages of MUX include high repeatability of data and its compact size.

### **Conclusion**

In this research project, an optical MUX was successfully developed as a cost effective, compact and reliable solution for multiple sensor testing needed to accelerate the sensor development process. The three-channel MUX is flexible such that it can be extended to more than three channels with relative ease. This method of optical multiplexing can be employed in any application that requires light from one source to be transferred to multiple destinations. The experiments in this research have demonstrated that light intensity is halved when it passes through a MUX channel, but the intensity of input light from an LED can be increased to achieve the desired output intensity. It was also determined that within three inches of a distance between the input and the output MUX channels, the efficiency of the MUX is not significantly affected. Moreover, the sensor data should be collected when the motor is in steady state. All these results make the optical MUX a useful device for optical multiplexing and demultiplexing applications.



## REFERENCES

1. E. W. Stein, P. S. Grant, H. Zhu, and M. J. McShane, "Microscale enzymatic optical biosensors using mass transport limiting nanofilms. 1. Fabrication and characterization using glucose as a model analyte," *Anal. Chem.* **79**(4), 1339-1348 (2007).
2. E. W. Stein, S. Singh, and M. J. McShane, "Microscale enzymatic optical biosensors using mass transport limiting nanofilms. 2. Response modulation by varying analyte transport properties," *Anal. Chem.* **80**(5), 1408-1417 (2008).
3. "MultiFrequency Phase Fluorometer." Retrieved 3/4/12, from <http://www.oceanoptics.com/products/mfpf100.asp>.
4. S. Haykin and B. V. Veen, *Signals and System*, Wiley 2nd ed., 430-431 (2005).
5. E. Hecht, *Optics*, 3rd ed., 162 (1997).
6. T. M. Bremer, S. V. Edelman, and D. A. Gough, "Benchmark data from the literature for evaluation of new glucose sensing technologies," *Diabetes technology & therapeutics* **3**(3), 409-418 (2001).
7. J. Hecht, *Understanding Fiber Optics*, 4th ed., 28, 97-100 (2001).

**CONTACT INFORMATION**

Name: Saadiah Gul Ahmed

Professional Address: c/o Dr. Michael J. McShane  
Department of Biomedical Engineering  
5045 Emerging Technologies Building  
Texas A&M University  
College Station, TX 77843

Email Address: saadiah\_gul@neo.tamu.edu

Education: BS Electrical Engineering,  
Texas A&M University, December 2012  
Undergraduate Research Scholar